e-Polymers **2008**, no. 060

http://www.e-polymers.org

ISSN 1618-7229

First application of electrosynthesized polyterthiophene to organic solar cells

M. Angélica del Valle,[1]* *Giovanny M. Soto*,[1] Luis I. Canales,[1] *Fernando R. Díaz*,[1] *J. Christian Bernède*[2]

[1*] Facultad de Química, P. Universidad Católica de Chile, V. Mackenna 4860, Santiago, Chile; fax: (56-2)6864744; e-mail: mdvalle@uc.cl
[2] Laboratoire des Matériaux Photovoltaïques (LAMP), Université de Nantes, BP 922008 Nantes cedex 3, France; fax: 02.51.12.55.28; e-mail: Jean-Christian.Bernede@univ-nantes.fr

(Received: 25 July, 2007; published: 18 April, 2008)

Abstract: Polyterthiophene (PTT) thin films have been electrosynthesized using potentiodynamic and potentiostatic methods. The optimal experimental conditions to prepare organic solar cells were determined by deposition of films on platinum and then the process was adapted to an indium tin oxide substrate. Surface morphology of films deposited by potentiostatic methods proved to be more homogeneous than films obtained by potentiodynamic methods. When PTT is employed in photovoltaic cells, the best results are attained using the latter technique. In these solar cells, the polymer is used as electron donor while N,N'-diheptyl-3,4,9,10-perylene-bis-carboximide (PTCDI-C7), deposited by vacuum sublimation, was the electron acceptor. The short circuit current is systematically small, probably due to the roughness of the polymer which induces high series resistance. In any case, it was demonstrated that the electrochemical method is suitable to prepare polymeric layers of electronic devices.

Introduction

The development of organic electronics during the last 15 years has induced a significant research effort to prepare new processable electroactive organic materials [1]. In the field of full organic solar cells, two families are found: devices based on bulk hetero-junctions [2, 3]; and devices based on multi-layer hetero-junctions of donor/acceptor materials [4, 5].

Conjugated polymers are promising materials to fabricate optoelectronic devices. They can be chemically synthesized and then processed by spin coating to produce thin film polymers to be used in organic devices. Another way to prepare them is by electrochemical methods that allow synthesizing the polymer directly onto glass substrates coated with a transparent conductive oxide (TCO) film, which is used as base electrode in organic devices. Such technique might be efficient to obtain devices based on multi-layer hetero-junctions. Moreover, the anodic polymerization method allows direct deposition of a polymer in its conductive *p*-doped state. Electrochemical polymerization presents interesting advantages such as direct deposition of the doped conducting polymer onto TCO substrates; easy control of the film thickness through the deposition charge; formation of films with good adhering and mechanical properties Besides, variables such as monomer concentration, solvent, electrolyte dopant nature and concentration, as well as the electrochemical

perturbation program (potentiostatic or potentiodynamic) can be controlled during the polymerization. All this makes possible to tailor the final polymer film material into a certain structure and morphology [6, 7].

Some thiophene derivatives have been tested in optoelectronic devices [3, 8, 9, 10], achieving good performance. As a rule, these derivatives bear bulky groups that play a very important role at polymerization time since such groups compromise the planarity of conjugated chains [11], having an influence on its conductivity. Consequently, although it is not a new material (its electrosynthesis is known for more than twenty years), TT is a material with promising properties to be employed as electron-donor in optoelectronic devices.

Likewise, polyterthiophene (PTT) has an advantage with regard to polymers obtained starting from five-membered heterocycles such as poly(thiophene). This advantage is its structure. Terthiophene is an oligomer of three units *i.e*. a trimer. This trimer contributes to make more ordered the oligomeric high density region (OHDR) formed by oligomers with different chain lengths. This is very important, as far as the determination of the types of nucleation and growth is concerned, in the polymerization mechanism of conducting polymers since the structure and morphology of electrochemically deposited polymer films are established by the OHDR composition. Therefore, it is necessary to control the variables governing the process (applied potential, electrolysis time, concentration, solvent, etc.), in order to control the OHDR [12–16].

In this research PTT films electrochemically synthesized by potentiostatic and potentiodynamic methods have been assayed as electron donor in photovoltaic cells. Previously, optimal conditions for the electrochemical synthesis adapted to films on glass as substrate and determination of the highest occupied molecular orbital (HOMO) were studied on platinum. The main goal of the present research is to establish the feasibility of utilizing electro-polymerization techniques for the elaboration of photovoltaic cells.

Results and discussion

Figure 1 shows the potentiodynamic *i/E* profiles registered within the range 0 - 1.18 V, perturbing the Pt/0.01 mol·L^{-1} TT + 0.10 mol·L^{-1} $TBAPF_6$ (in acetonitrile) interface. Electro-oxidation and polymerization of TT, as well as the redox processes associated with the polymer film, are depicted. The observed voltammetric behaviour is similar to that obtained for thiophene in similar conditions (Pt/ 0.10 mol·L^{-1} thiophene + 0.50 mol·L^{-1} $TBAPF_6$ in acetonitrile) [9]. The most relevant difference between both profiles is the electro-oxidation potential, *i.e*., lower for TT because the polymerization process occurs from a trimer. As it is known increase of length in the polymer chain leads to a decrease of the oxidation potential, owing to a higher electronic delocalization (level decay of the corresponding HOMO) [17, 18]:

$$E_{monomer} > E_{dimer} > E_{trimer} > E_{oligomer} > E_{polymer}$$

As the number of voltammetric cycles increases, a dark blue compact film is formed on the electrode, giving rise to the polymerization process, due to oxidation observed at *ca*. 1.1 V. Current increases on successive potentiodynamic scans, and anodic and cathodic peaks are also developed, which may be associated to redox charge-discharge (doping-undoping) process of the deposited PTT film.

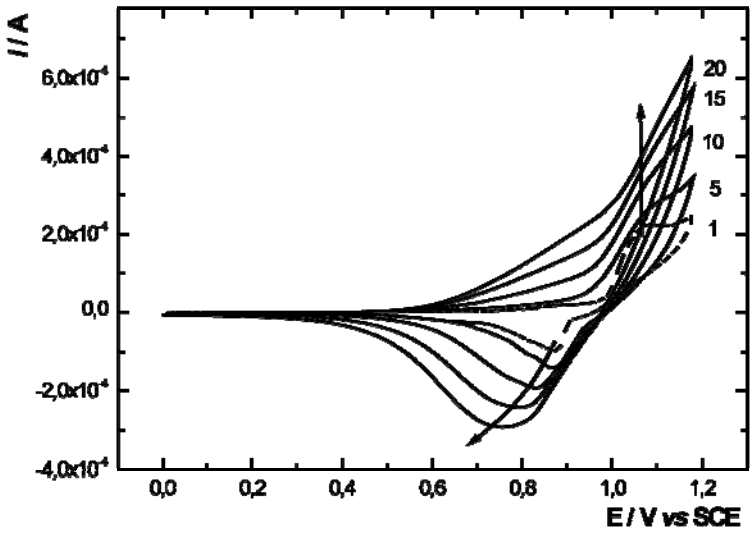

Fig. 1. Successive i / E profiles (*current, in Amp vs potential, in V refered to SCE)* of TT from cycle 1 (---) to 20 (—) on Pt electrode. Scan rate, v, 8 $mV \cdot s^{-1}$ (0.01 $mol \cdot L^{-1}$ TT + 0.1 $mol \cdot L^{-1}$ $TBAPF_6$ in CH_3CN).

Figure 2 shows the *i*-t transient for the electro-polymerization of TT at the Pt/0.01 $mol \cdot L^{-1}$ TT + 0.1 $mol \cdot L^{-1}$ $TBAPF_6$ (in acetonitrile) interface. After the double layer is charged, the current drops to a minimum after a time τ (induction time) and then increases. The current drop follows a $i \times t^{-1/2}$ (Cottrell) relationship, corresponding to a diffusion-controlled process. In previous works [13, 15, 19, 20], this process has been ascribed to oxidation of the monomer units diffusing from the solution, wherein the oligomerization process occurs and the OHDR is established. Once this region reaches oversaturation, at time τ, the polymerization process begins.

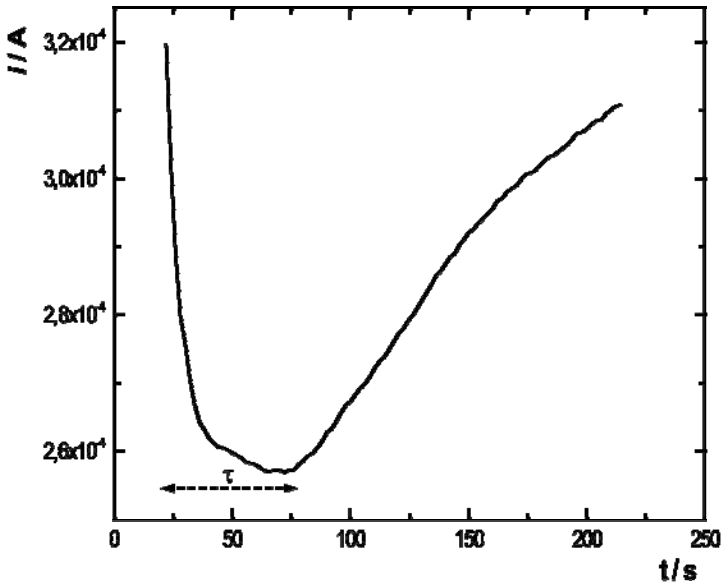

Fig. 2. j/t transient obtained during TT polymerization on Pt electrode by potentiostatic method. E = 1.18 V; 0.01 M TT + 0.1 M $TBAPF_6$ in CH_3CN.

Two main differences are found when *i-t* transients of TT and thiophene are compared [13]. Firstly, the induction time is larger for TT, which may indicate that the nucleation process starts from larger chain oligomers, therefore the OHDR might be

more ordered. The other outstanding difference is the absence of the second current step: thiophene in acetonitrile (conditions mentioned above) shows two current steps, the second current step being associated to the deposition of a second layer of the polymer [13].

Figure 3 depicts the electrochemical *p*-doping/undoping process of PTT in the electrolytic solution. A reversible redox, doping/undoping process is observed, which can be inferred from values listed in Table 1, because the ratio Q_+/Q_- is *ca*. 1.

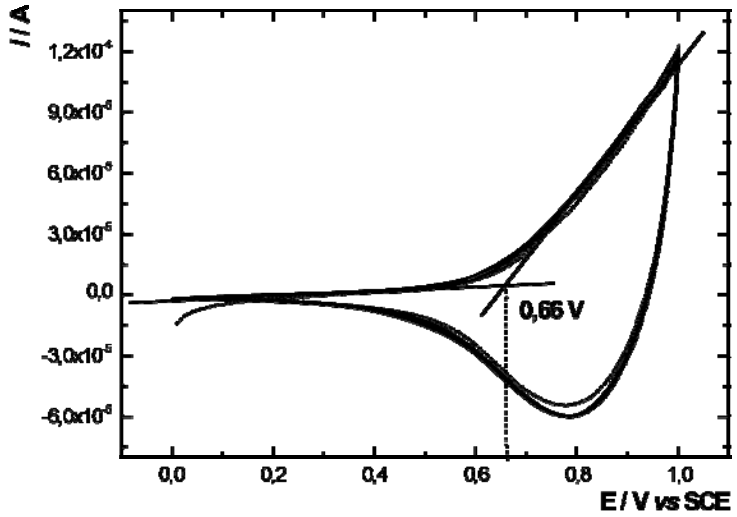

Fig. 3. j / E of PTT deposited on Pt electrode in 0.1 $molL^{-1}$ $TBAPF_6$., from cycle 1 (---) to 5 (—), v = 8 $mV \cdot s^{-1}$.

Tab. 1. *p*-doping/undoping charges (Q_+/Q_-) obtained from Fig. 3.

scan Nº	Q_+ (C)	Q_- (C)	Q_+/Q_-
1	$2.30 \cdot 10^{-3}$	$2.18 \cdot 10^{-3}$	1.06
5	$2.44 \cdot 10^{-3}$	$2.49 \cdot 10^{-3}$	0.98

The *p*-doping (E_p) and *n*-doping (E_n) potentials can be used to determine the highest occupied molecular orbital (HOMO) and lowest unoccupied molecular orbital (LUMO) energy levels of conducting polymers [21–24], and the potential difference ($\Delta E = E_p - E_n$) can be used to estimate the energy gap of the polymer ($E_g = e\,\Delta E$). According to Leeuw *et al.* [21], the energy levels (in electron volts, eV) corresponding to the electrochemical potentials can be obtained by adding 4.4 V to the potentials. Then, $E_{HOMO} = -e(E_p + 4.4)$, and $E_{LUMO} = -e(E_n + 4.4)$, where E_{HOMO} and E_{LUMO} are the energy levels of HOMO and LUMO respectively.

Therefore, from Fig. 3,

$$E_{HOMO} = -e(E_p + 4.394) = -5.054 \text{ eV} \quad (1)$$

Unfortunately, E_{LUMO} cannot be calculated since the electrochemical *n*-doping/undoping obtained was very weak or nil. Consequently, E_{LUMO} was calculated using the energy gap obtained by absorbance measurements. Figure 4 shows the absorbance spectrum of PTT potentiostatically deposited in its doped state. It can be seen that the transmission curve exhibits threshold energy of *ca*. 2.03 eV. It can be

roughly estimated that this threshold energy corresponds to the optical band gap of PTT. Therefore, considering that E_{HOMO} - E_{LUMO} = - E_{gap}, E_{LUMO} can be estimated as:

$$E_{LUMO} = 2.03 + (-5.05) = -3.02 \text{ eV} \quad (2)$$

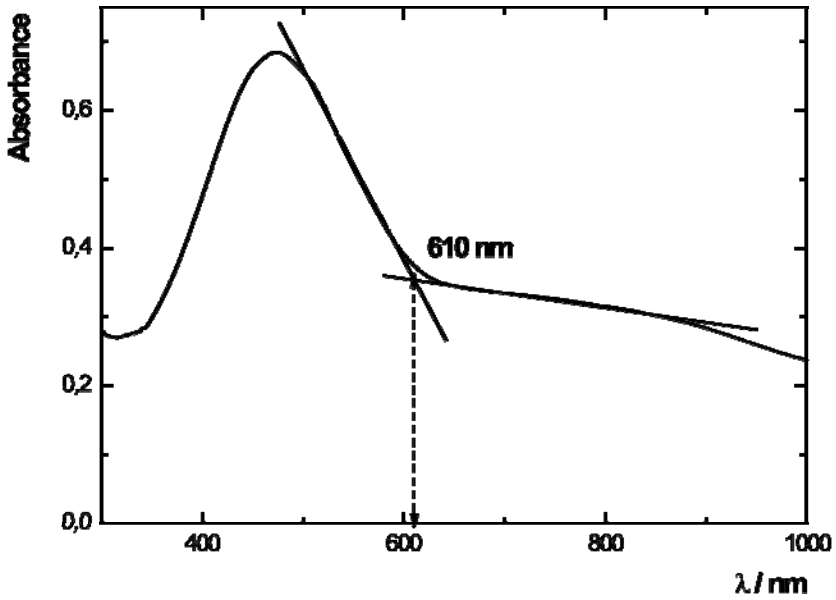

Fig. 4. Absorption spectrum of PTT obtained as in Fig. 2, by the potentiostatic method.

After demonstrating that polythiophene is a material having a suitable band-gap to be utilized as electron-donor, Fig. 5, and based upon previous studies about the optimum electro-synthesis working conditions on Pt, further extrapolated to ITO, photovoltaic cells were manufactured with the following structure:

ITO/PTT/PTCDI-C7/LiFAl/P

where *ITO* was used as TCO; PTT (electron donor) obtained in its doped or undoped state when electrolized by potentiostatic or potentiodynamic methods, respectively; PTCDI-C7 (electron acceptor) [25]; LiF is used to improve the fill factor (FF) and open circuit voltage (V_{oc}) [26]; Al is the electrode and P is a protector layer of the organic/Al interface [27].

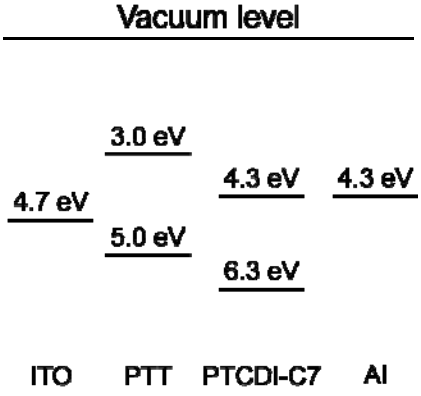

Fig. 5. Energy diagram of ITO/PTT/PTCDI-C7/LiFAl/P solar cell.

Typical J - V characteristics obtained under AM 1.5 illumination for cells differing only in the method employed to synthesize the polymer layer, is shown in Fig. 6. It can be observed that the J - V shape of these characteristics exhibit a "reverse bowing" with very small FF. The short circuit current, I_{sc}, is also quite small. It seems that, in general, the performance of photovoltaic in which the polymer has been deposited by cyclic voltammetry, is better than that with PTT potentiostatically synthesized. In fact, not only I_{sc} is higher, but so is the open circuit voltage (V_{oc}).

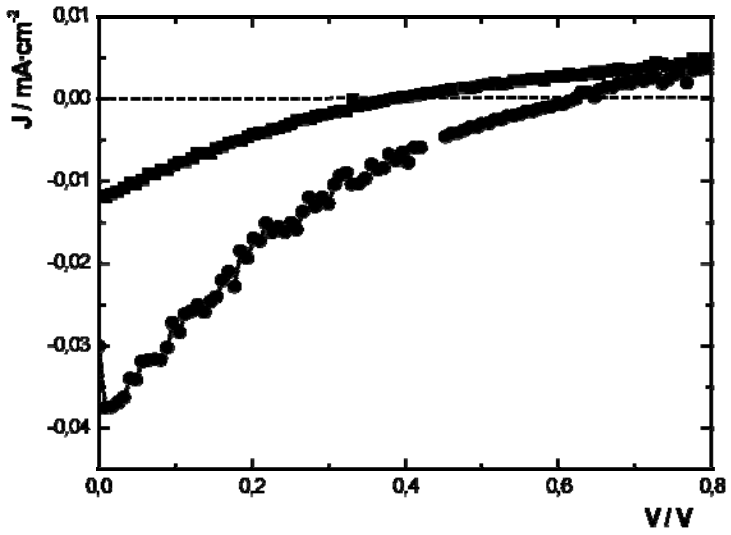

Fig. 6. j–V characteristics under AM 1.5 illumination of glass/ITO(100nm)/PTT (420nm)/PTCDI-C7(25nm)/LiF(2nm)Al(80nm)/P. Polymer deposited either by cyclic voltammetry (10 cycles) (●), or potentiostatically (3 min) (■).

Often small I_{sc} and FF are attributed to high series resistances, R_s, while small open circuit voltage are often ascribed to small shunt resistance, R_{sh}. High R_s values can be induced by small carrier mobility in the organic material and/or to high contact resistance.

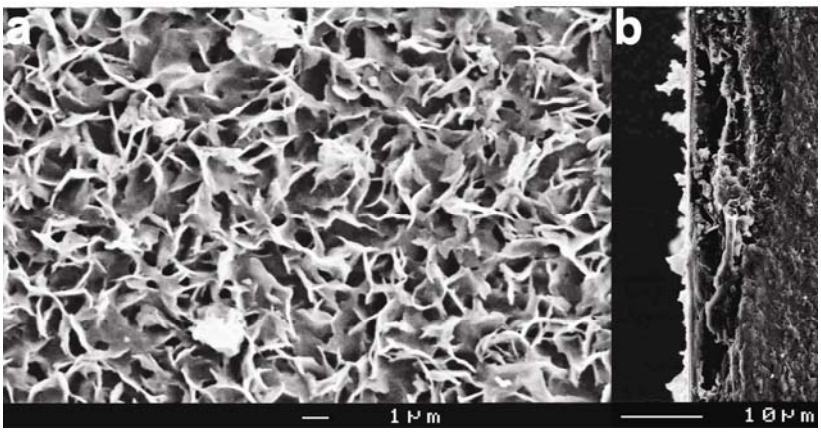

Fig. 7. SEM micrographs of PTT obtained by cyclic voltammetry as in Fig. 1. (a) film surface; (b) cross section.

Surface morphology and the cross section of a PTT film deposited by cyclic voltammetry are displayed in Fig. 7. It can be observed that the films are highly inhomogeneous. Structures perpendicular to the substrate surface are randomly distributed over the film surface. They may reach up to 3 μm in height. Between them a thin layer, thickness *ca*. 400 nm, is clearly visible. Consequently, in that cell, the PTT thickness, *X,* varies between 400 nm and 3 μm. It is clear that the active part of the film in PV-cells corresponds to the thin layer. The structures described above are too thick to allow any carrier collection. Therefore, such morphology should induce inhomogeneous interface contact with Al and therefore large series resistance, which might lead to small FF and short circuit current.

Figure 8 shows that films deposited by potentiostatic methods are more homogeneous. In addition, the thickness of the film (200 nm) is smaller than that obtained by potentiodynamic methods. Therefore, the contact resistance induced by such homogeneous films should be smaller than that induced by the rough surface of films deposited by cyclic voltammetry. However, devices using this family of films exhibit the smallest I_{sc} and poor FF.

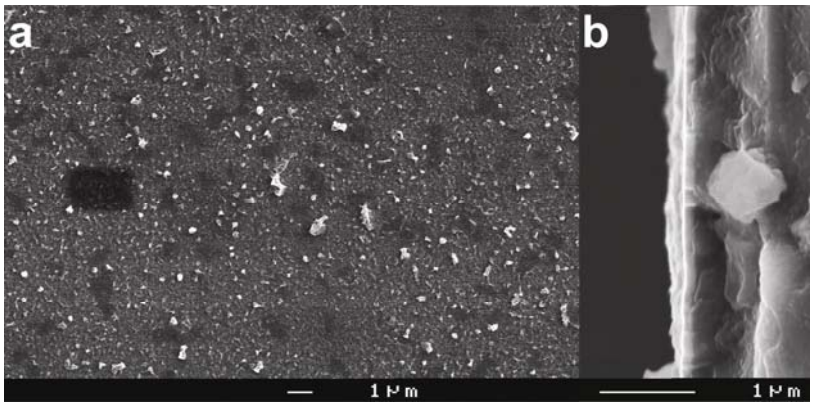

Fig. 8. SEM micrographs of PTT obtained by potentiostatic means as in Fig. 2. (a) film surface; (b) cross section.

It is known that the order of polymer chains synthesized by voltammetry is higher than that obtained by potentiostatic processes [17], therefore the carrier mobility is higher in the former case which accounts for the smaller series resistance and, consequently, better cell performance.

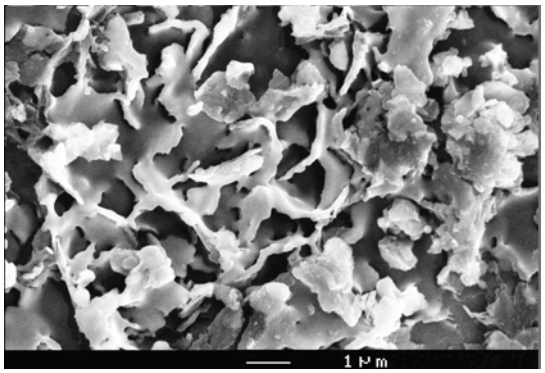

Fig. 9. SEM micrograph of PTT/PTCDI-C7/LiFAl/P cell. Visualization of the memory effect of the polymer roughness.

However, even if films synthesized by voltammetry were more ordered, their roughness induces poor quality interface. It can be seen in Fig. 9 that, even after cell capping with selenium layers, there is a "memory effect" of the roughness of the polymeric film.

Conclusions

PTT thin films have been electrochemically polymerized, either by potentiodynamic (0 - 1.18 V) or potentiostatic (1.2 V) methods. From the absorbance spectrum, the band gap of the polymer was estimated as 2.03 eV. The HOMO value, -5.05 eV, has been calculated from the results obtained by cyclic voltammetry. Therefore, from the HOMO and band gap values, a LUMO value of -3.02 eV was worked out. PTT was tried out as electron donor in solar cells, the acceptor being PTCDI-C7 deposited by vacuum sublimation. A photovoltaic effect was displayed whether the electrochemical method used to prepare the polymeric layer was potentiostatic or potentiodynamic. Nevertheless, the best results were obtained when the films were deposited by cyclic voltammetry. It is assumed that these films are more ordered, which would justify the higher carrier mobility. However, as SEM showed, the surface of these films is very rough, which explains the small collected current. It seems that, in the future, the voltammetric deposition process should be improved in order to obtain a suitable film surface morphology that allows obtaining more efficient solar cells. In any case, it was demonstrated that the electrochemical method is suitable to prepare polymeric layers of electronic devices.

Experimental

2,2',5',2"-terthiophene (TT) monomer, tetrabutylammonium hexafluorophosphate ($TBAPF_6$), and anhydrous acetonitrile were purchased from Aldrich and used as received. The electrochemical experiments were carried out in a three-compartment three-electrode glass cell. A Pt gauze of large geometrical area and a Ag/AgCl in tetramethylammonium chloride (Me_4NCl) were used as counter and reference electrodes, respectively. All the potentials quoted in this work are referred to the saturated calomel electrode (SCE) [28]. The electron donor polymer utilized in the ITO/PTT/PTCDI-C7/LiFAl/P cells was electrochemically synthesized either by cyclic voltammetry sweeping between 0 to 1.18 V (Pt); and 0 to 1.2 V (TCO) at 8 $mV \cdot s^{-1}$ or by the potentiostatic method (transient i-t at 1.18 V on Pt; and 1.2 V on TCO during 3 minutes). Poly(2,2',5',2"-terthiophene) was deposited on an ITO electrode (*ca*. 1.5 cm^2) from a solution containing 10^{-3} $mol \cdot L^{-1}$ TT + 0.1 $mol \cdot L^{-1}$ $TBAPF_6$ in anhydrous acetonitrile, while for the electrochemical measurements of p-doping and n-doping potentials, PTT was deposited onto a Pt disc electrode (0.07 cm^2 geometric area) from a solution containing 10^{-2} $mol \cdot L^{-1}$ TT + 0.1 $mol \cdot L^{-1}$ $TBAPF_6$ in anhydrous acetonitrile. To warrant a minimum content of water in all experiments (below 0.5 $mmol \cdot L^{-1}$) acetonitrile was stored under dry argon atmosphere, on molecular sieves (3 Å), and handled with a syringe. p- and n-doping potentials were measured in anhydrous MeCN using 0.1 $mol \cdot L^{-1}$ $TBAPF_6$ as supporting electrolyte. It is noteworthy to mention that the previous characterization was performed using Pt as working electrode. This is necessary because constant surface area must be granted and this is quite difficult to achieve on indium tin oxide, ITO. Once the optimum working conditions have been established, ITO is employed as substrate since this is the material suitable for the fabrication of the optoelectronic device.

The experiments were performed on a Radiometer (Model PGP201) potentiostat interphased to a computer for data acquisition and analysis.

A TCO coated glass was used as substrate for the fabrication of PTT/PTCDI-C7/LiFAl/P cells. The TCO electrode was a layer of ITO on a 10·25 mm^2 glass substrate. ITO substrate was supplied by SOLEMS. The whole glass substrate was coated; therefore some ITO must be removed to obtain the electrode. After masking a 10·10 mm^2 band, ITO was etched using Zn + HCl as etchant [29]. Then, the substrate was cleaned by using the H_2O_2 treatment described by Osada et al. [30]. The substrate was treated with a H_2O-H_2O_2 (30%) – NH_4OH (25%) solution (5:1:1) at 80 °C for 20 min and finally rinsed with boiling water for 5 min. The use of boiling water is useful for obtaining impurity-free surfaces. After rinsing the ITO electrode, the polymer was electro-synthesized as described above. Next, N,N'-diheptyl-3,4,9,10-perylene-bis-carboximide (PTCDI-C7) was deposited using vacuum deposition under a pressure of 10^{-4} Pa. The thin film deposition rate and thickness were estimated *in situ* by means of a quartz monitor: 0.05 – 0.07 $nm \cdot s^{-1}$ and 25 nm, respectively, for PTCDI-C7. The thickness was chosen after optimization. The thickness of the organic films was checked by SEM.

After the organic thin film deposition, LiF/aluminium upper electrodes were thermally evaporated, without breaking the vacuum, through a mask 1.5 x 6 mm active area. The LiF layer was 2 nm thick, and that of Al 80 nm. After breaking the vacuum five minutes, an encapsulating layer, *ca*. 70 nm thick, of amorphous selenium (Se-a), was thermally evaporated. The amorphous selenium layer has proved to be very efficient to protect the under layers from oxygen and water vapour contamination [31], avoiding thus the fast degradation of the devices. Moreover, it has been shown recently that when the aluminium cathode remains five minutes in contact with room air before encapsulation, there is an increase of the open circuit voltage, and efficiency values are ascribed to the formation of a thin alumina layer at the organic acceptor/aluminium interface [27]. Therefore, the structure used was glass/ITO (100nm)/ PTT(X)/PTCDI-C7(25nm)/LiF (2nm)Al(80nm)/P.

The optical measurements were performed at room temperature on a Carry spectrometer. The optical density was measured at wavelengths 2 – 0.25 μm.

The surface topography and cross section of the films were observed with a field emission scanning electron microscope (SEM, JEOL F-6400). Film thickness was measured from the cross section visualization using simple software.

Electrical characterization of the cells was performed with an automated I-V tester; in the dark and under 1 sun global AM 1.5 simulated solar illumination.

Acknowledgements

This work has been financially supported by Fondecyt 1060598 and ECOS-CONICYT C05E10 grants.

References

[1] Bernède, J. C.; Jousseaume, V.; del Valle, M. A.; Díaz, F. R. *Current Trends Pol. Sci*. **2001**, *6*, 135.
[2] Brabec, C.; Dyakonov, V.; Parisi, J.; Sariciftci, N. S. "Organic Photovoltaics –Concepts and Realization", Mat. Sci. 60, Springer, Berlin, **2003**.
[3] Brabec, C. J. *Sol. Energy Mater. Sol. Cells* **2004**, *83*, 273.

[4] Peumans, P.; Forrest, S. R. *Appl. Phys. Lett*. **2001**, *79*, 126.
[5] Peumans, P.; Yakimov, A.; Forrest, S.R. *J. Appl. Phys*. **2003**, *93*, 3693.
[6] Lincot, D. *Thin Solid Films* **2005**, *487*, 40.
[7] Ugalde, L.; Bernède, J. C.; del Valle, M. A.; Díaz, F. R.; Leray, P. *J. Appl. Pol. Sci*. **2002**, *84*, 1799.
[8] Brabec, C. J.; Sariciftci, N. S.; Hummelen, J. C. *Adv. Funct. Mater.* **2001**, *11*, 15.
[9] Hou, J.; Yang, C.; Li, Y. *Synth. Met*. **2005**, *153*, 93.
[10] Liu, P.; Wang, X.; Zhang, Y.; Zhou, X.; Deng, W. *Synth. Met*. **2005**, *155*, 565.
[11] Mårdalen, J.; Fell, H .J.; Samuelsen, E. J.; Bakken, E.; Carlsen, H. J.; Andersson, M. R. *Macromol. Chem. Phys.* **1995**, 196, 553.
[12] del Valle, M. A.; Ugalde, L.; Díaz, F. R.; Bodini, M. E.; Bernède, J. C.; Chaillou, A. *Polym. Bull*. **2003**, *51*, 55.
[13] del Valle, M. A.; Cury, P.; Schrebler, R. *Electrochim. Acta* **2002**, *48*, 397.
[14] del Valle, M. A.; Ugalde, L.; del Pino, F.; Díaz, F. R.; Bernède, J. C. *J. Braz. Chem. Soc*. **2004**, *15*, 272.
[15] Schrebler, R.; Grez, P.; Cury, P.; Veas, C.; Merino, M.; Gómez, H.; Córdova, R.; del Valle, M. A. *J. Electroanal. Chem*. **1997**, *430*, 77.
[16] del Valle, M. A.; Díaz, F. R.; Bodini, M.; Alfonso, G.; Soto, G. M.; Borrego, E. D. *Polym. Int*. **2005**, *54*, 526.
[17] Simonet, J.; Rault-Berthelot, J. *Prog. Solid State Chem*. **1991**, *21*, 1.
[18] Eales R. M.; Hillman A. R. *J. Electroanal. Chem.* **1988**, *250*, 219.
[19] Bade, K.; Tsakova, V.; Schultze, J. W. *Electrochim. Acta* **1992**, *37*, 157.
[20] Hillman, A. R.; Mallen, E. F. *J. Electroanal. Chem*. **1988**, *243*, 403.
[21] de Leeuw, D. M.; Simenon, M. M. J.; Brown, A. R.; Einerhand, R. E. F. *Synth. Met.* **1997**, *87*, 53.
[22] Eckhardt, H.; Shacklette, L. W.; Jen, K. Y.; Elsenbaumer, R. L. *J. Chem. Phys*. ***1989***, *91*, 1303.
[23] Cervini, R.; Li, X.-C.; Spencer, G. W. C.; Holmes, A. B.; Moratti, S. C.; Friend, R. H. *Synth. Met*. **1997**, *84*, 1277.
[24] Li, Y.; Cao, Y.; Cao, J.; Wang, D.; Yu, G.; Heeger, A. J. *Synth. Met*. **1999**, *99*, 243.
[25] Berredjem, Y.; Karst, N.; Cattin, L.; Lakhdar-Toumi, A.; Godoy, A.; Soto, G.; Diaz, F.; del Valle, M. A.; Morsli, M.; Drici, A.; Boulmokh, A.; Gheid, A. H.; Khelil, A.; Bernède, J. C. *Dyes and Pigments*; article in press, available online.
[26] Brabec C. J.; Shaheen S. E.; Winder C. Sariciftci N. S. *Appl. Phys. Lett.* **2002**, 80, 1288.
[27] Karst, N.; Bernède, J. C. *Phys. Sol. (a)* **2006**, *203*, R70.
[28] East, G. A.; del Valle, M. A. *J. Chem. Ed*. **2000**, *77*, 97.
[29] Gordon, R. G. *Mater Res. Soc. Symp. Proc*. **1996**, 426:419.
[30] Osada, T.; Kugler, Th.; Bröms, P.; Salanek, W. S. *Synth. Met*. **1998**, *96*, 77.
[31] Latef, A.; Bernède, J. C. *Phys. Stat. Sol*. *(a)* **1991**, *124*, 243.